

Non-newtonian flow modelling based design of plate heat exchangers

Abhishek R. Joshi, A. K. Datta*

(Agricultural and Food Engineering Department, IIT Kharagpur, West Bengal-721 302, India)

Abstract: Plate heat exchangers (PHEs) are widely used in food industries for processing liquid products, because of their high thermal effectiveness, ease of maintenance and cleaning, high heat exchange rate and demand of relatively small floor area. As many food products are non-Newtonian fluids, particularly pseudoplastic in nature, it is important to study nature of their flow and heat transfer characteristic in PHEs. Aqueous solutions of carboxymethylcellulose (CMC) at different weight concentrations (0.2%, 0.4% and 0.6%) and $25 \leq N_{Re,gen} \leq 250$ and at different inlet temperatures (50 °C, 60 °C and 70 °C) were considered as operating conditions. Using data obtained, relations between dimensionless numbers (N_{Nu} , N_{Pr} and $N_{Re,gen}$) were established. Pressure drop across inlet and outlet of PHE was measured for each run and correlations between friction factor and generalized Reynolds number were established for different concentrations. To study flow pattern of CMC fluid through narrow gap between two plates, simulation was carried out using FLUENT 6.3 software by supplying actual experimental conditions. Theoretical method is suggested for predicting temperatures of fluids after each pass of PHE.

Keywords: non-Newtonian fluids, heat transfer, plate heat exchanger, flow simulation

Citation: Joshi, A. R., and A. K. Datta. 2017. Non-newtonian flow modelling based design of plate heat exchangers. *Agricultural Engineering International: CIGR Journal*, 19(1): 195–204.

1 Introduction

Plate heat exchangers (PHEs) are used extensively in the food and dairy industries, but very little basic information has been published on their flow and heat transfer characteristics. Advantages of these over other heat exchangers are flexibility of flow arrangements, high heat transfer rates, and ease of opening for cleaning and sanitary requirements. PHEs are generally used in food processing industry for cooling and heating applications in milk and citrus juices, tropical fruit pulp pasteurization, concentration processes, etc.

Corrugated surfaces of plate heat exchangers serve as turbulence promoters to increase local heat and mass transfer rates. These are broadly used in food industries where the two main purposes are to avoid the burnout of the fluid because of the heterogeneity of the heat transfer

to the wall and to allow a good mixing of the fluid (Gradeck et al., 2005). Many different plate surface corrugation patterns are employed in PHEs that essentially promote enhanced heat transfer (Muley et al., 1999). Heat transfer between a surface and an adjacent flow may be characterized by the value of a local film coefficient, which depends on the flow regime and on the structure of the surface adjacent to fluid. This structure is involved in the shear rate value at the wall. Heat and mass transfer rates are governed by the shape of the heat exchange surface and the rheological behaviour of the fluid (Bereziatec and Devienne, 1999).

A large number of fluid foods, such as ice cream mix, condensed milk, tomato catsup, etc., exhibit non-Newtonian behaviour, which means these do not exhibit a direct proportionality between shear stress and shear rate. One of the most popular models is the Ostwald–De Waele model, given by Equation (1), which is also known as the power-law model.

$$\tau = K(\dot{\gamma})^n \quad (1)$$

where, τ is shear stress, Pa; K is consistency coefficient,

Received date: 2016-07-14 Accepted date: 2016-12-13

* Corresponding author: A. K. Datta, Agricultural and Food Engineering Department, IIT Kharagpur, West Bengal-721 302, India. Email: akdiitkgp@gmail.com. Tel: +919051309591.

Pa s^n ; $\dot{\gamma}$ is shear rate, $\text{m m}^{-1} \text{s}^{-1}$; n is flow behavior index, dimensionless.

It is important to consider non – Newtonian behaviour of food materials as these follow different flow patterns and heat transfer characteristics, as compared to Newtonian fluids because of apparent viscosity, which is shear-rate-dependent. Mathematical models for heat transfer and pressure drops are required for the design and sizing of PHEs. For heat exchangers, the convective heat transfer coefficient is commonly obtained from correlations among Nusselt, Reynolds and Prandtl dimensionless numbers (Kumbhare and Dawande, 2013). Furthermore, the friction factor is commonly correlated with Reynolds number. In case of thermal processing of liquid foods, the model must also take non-Newtonian behaviour into account through consistency and flow behaviour indices (Carla et al., 2007).

The objectives of this study are:

- i) to study the heat transfer characteristic of non – Newtonian fluids in a laboratory model PHE in order to obtain film coefficients in terms of dimensionless parameters;
- ii) to obtain friction factors in terms of generalised Reynolds number for the same fluids; and
- iii) to study flow behaviour of non-Newtonian fluids through PHE using simulation technique based on FLUENT 6.3 software.

2 Materials and methods

Aqueous solutions of Carboxy Methyl Cellulose (CMC) were used to obtain non-Newtonian fluids.

Different concentrations in water led to different nature of fluids (variation in flow behaviour index and consistency coefficient). In this study 0.2%, 0.4% and 0.6% (w w⁻¹) concentrations have been used (Kumar, 2006). CMC solutions with different flow rates passed through PHE at different inlet temperatures. The other (cold) fluid was water with constant flow rate for all the runs.

PHE used for this study was of two pass – series type meaning two pass for cold water and series pass for hot water (Table 1). Figure 1 shows the experimental setup of the PHE while the fluid flow pattern is presented in Figure 2.

Table 1 Plate dimensions & details

Components	Dimensions
Number of plates	13
Length and height	730 mm and 75 mm
Width	200 mm
Thickness	1.2 mm
Gap between plates	5 mm
Chevron angle	90°
Plate material	Stainless steel

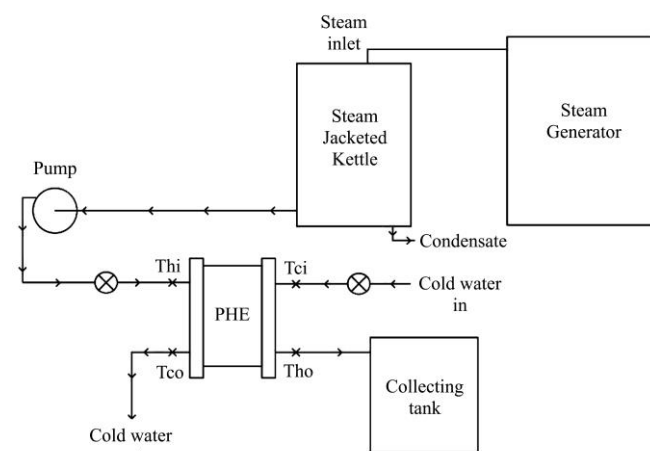


Figure 1 Experimental setup of PHE

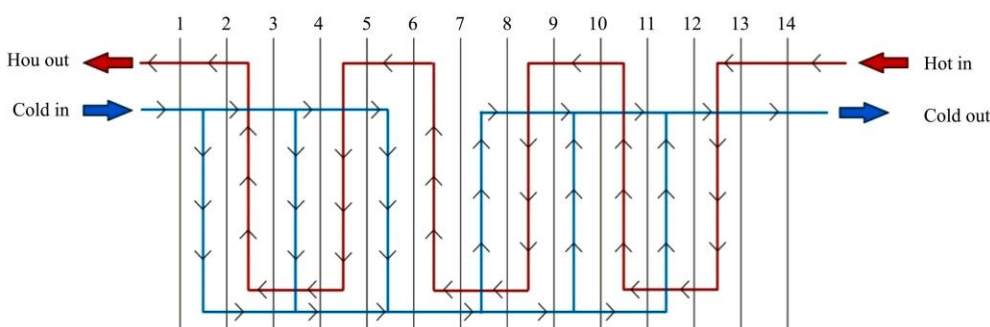


Figure 2 Arrangement of flow patterns in PHE

For 6C (countercurrent)-5P (parallel) flow arrangement; correction factor (F) for LMTD had to be calculated. For that both primary and secondary fluids

used were water only. Flow rate of secondary fluid was kept constant throughout the experiment (30 L min^{-1}). For particular flow rate of primary fluid, variation in

temperatures at inlet & outlet were recorded. F values were calculated for different flow rates & inlet temperatures of primary fluid. Heat dissipation from the hot fluid is expressed in Equation (2):

$$\dot{Q}_h = (\dot{q}_h \times \rho_h) \times C_{ph} \times (T_{hi} - T_{ho}) \quad (2)$$

where, \dot{Q}_h is the thermal power dissipated from the hot fluid, W; \dot{q}_h is the volume flow rate of the hot fluid, $\text{m}^3 \text{s}^{-1}$; ρ_h is the mean density of the hot fluid, kg m^{-3} ; C_{ph} is the specific mean heat capacity of the hot fluid, $\text{J kg}^{-1} \text{K}^{-1}$; T_{hi} is the inlet temperature of the hot fluid, $^{\circ}\text{C}$; T_{ho} is the outlet temperature of the hot fluid, $^{\circ}\text{C}$.

The same power dissipation can be equated to the product of overall heat transfer coefficient, log-mean temperature difference, area of indirect heat exchange and correction factor, as given in Equation (3):

$$\dot{Q}_h = F \times U \times A_h \times \Delta T_{lm} \quad (3)$$

where, F is the temperature correction factor, dimensionless; U is the overall heat transfer coefficient, $\text{W m}^{-2} \text{K}^{-1}$; A_h is the area of indirect heat exchange, m^2 ; ΔT_{lm} is the log-mean temperature difference, $^{\circ}\text{C}$.

The same experiments were performed by replacing primary fluid (hot) water with CMC solutions having different concentration each time. F value was used to obtain overall heat transfer coefficient. The latter can be related to the hot and cold fluids' film coefficients and metal thermal conductivity as per Equation (4) and Equation (5):

$$\frac{1}{U} = \frac{1}{h_h} + \frac{t}{k_m} + \frac{1}{h_c} \quad (4)$$

$$N_{Nuh} = \frac{h_h \times D_h}{k_h} \quad (5)$$

where, h_h is the film coefficient for the hot fluid, $\text{W m}^{-2} \text{K}^{-1}$; h_c is the film coefficient for the cold fluid, $\text{W m}^{-2} \text{K}^{-1}$; k_m is the thermal conductivity of the stainless steel plates, $\text{W m}^{-1} \text{K}^{-1}$; k_h is the thermal conductivity of the hot fluid, $\text{W m}^{-1} \text{K}^{-1}$; D_h is the effective hydraulic diameter of the channel carrying the hot/cold fluids, m; N_{Nuh} is the Nusselt number for the hot fluid, dimensionless.

The secondary fluid was water, for which the convective heat transfer coefficient h_c was calculated as per the following variant of Dittus-Boelter equation

(Equation (6) and Equation (7)), as supplied by the manufacturer of the PHE:

$$N_{Nuc} = \frac{h_c \times D_h}{k_c} \quad (6)$$

$$N_{Nuc} = 0.28 N_{Re}^{0.65} N_{Pr}^{0.4} \quad (7)$$

where, N_{Nuc} is the Nusselt number for the cold fluid, dimensionless; h_c is the convective (film) heat transfer coefficient of the cold fluid, $\text{W m}^{-2} \text{K}^{-1}$; k_c is the thermal conductivity of the cold fluid, $\text{W m}^{-1} \text{K}^{-1}$; N_{Re} is the Reynolds number, dimensionless; N_{Pr} is the Prandtl number, dimensionless.

N_{Re} and N_{Pr} are based on properties of Newtonian liquid, channel geometry and average velocity of the cold fluid in the channel. For calculating N_{Re} & N_{Pr} for non-Newtonian fluid flow through narrow channel, following relations, as given in Equation 8 and Equation 9, were used (Datta, 2001):

$$N_{Re_{gen}} = \frac{4 \times v_h^{2-n} \times \rho_h \times \delta^n}{3^{n-1} \times K \times \left(\frac{2n+1}{3n}\right)^n} \quad (8)$$

$$N_{Pr_{gen}} = \frac{C_{ph} \times K \times \left(\frac{2n+1}{3n}\right)^n \times \left(\frac{3v_h}{\delta}\right)^{n-1}}{k_h} \quad (9)$$

where, $N_{Re_{gen}}$ is the generalized Reynolds number, applicable for non-Newtonian liquids, dimensionless; $N_{Pr_{gen}}$ is the generalized Prandtl number, applicable for non-Newtonian liquids, dimensionless; V_h is the average velocity of flow for the hot fluid, m s^{-1} ; δ is the half gap width of the rectangular channels, formed by the PHE, m.

As evident, the two dimensionless Numbers $N_{Re_{gen}}$ and $N_{Pr_{gen}}$ are dependent on thermal and rheological properties of non-Newtonian liquids apart from the channel geometry and average velocity through the channel.

Pressure drop across plate heat exchanger is given by Equation (10):

$$\Delta P = \frac{2 \times f \times \rho_h \times L \times v_h^2}{D_h} \quad (10)$$

where, ΔP is the pressure drop, Pa; f is the Fanning friction factor for rectangular channel flow, dimensionless; L is the length of passage through the channels, m.

If pressure drop is known, one can estimate the

theoretical pumping capacity (power) required to pump the fluid through plate heat exchanger, as per Equation (11):

$$PS = \Delta P \times \dot{q}_h / 735.5 \quad (11)$$

where, *PS* is the metric horse power, Pferdestarke.

Dimensionless Nusselt Number can be expressed in terms of dimensionless generalized Reynolds Number and Prandtl Number (Carla et al., 2007) for non-Newtonian fluids as in Equation (12):

$$N_{Nuh} = a(N_{Re,gen})^b (N_{Pr,gen})^{0.33} \quad (12)$$

Similarly, the friction factor *f* can be expressed in terms of generalized Reynolds Number as per Equation (13):

$$f = c(N_{Re,gen})^d \quad (13)$$

Here, *a*, *b*, *c* and *d* are empirical constants.

3 Results and discussion

Table 2 lists the convective heat transfer coefficients applicable to hot and cold water flowing through the PHE as per Equation (7). Equation (7) was used for both hot and cold liquids as this was the recommended correlation among *N_{Nuh}*, *N_{Re}* and *N_{Pr}*, as per the manufacturer’s (APV Limited) literature. The *F* values obtained ranged from 0.5329 to 0.7815 with a mean of 0.70 and standard deviation of 0.074. Hence, 0.7 was taken as the mean log – mean temperature correction factor for the plate heat exchanger and this was used for non-Newtonian fluids (CMC solutions, flowing as hot liquid).

Table 2 F values as obtained from application of Equation (3)

<i>T_h</i> , °C	<i>h_h</i> , W m ⁻² K ⁻¹	<i>h_c</i> , W m ⁻² K ⁻¹	<i>U</i> , W m ⁻² K ⁻¹	<i>Q_h</i> , kW	<i>F</i>
Hot solution: 25 L min ⁻¹ , Cold water: 30 L min ⁻¹					
70	7190	5110	2411	34.6	0.7326
60	7018	5110	2391	24.8	0.7656
50	6651	4959	2315	16.7	0.7815
Hot solution: 12 L min ⁻¹ , Cold water: 30 L min ⁻¹					
70	6219	5110	2291	30.1	0.7198
60	7018	4959	2358	25.8	0.6884
50	5753	4959	2196	14.0	0.5329
Hot solution: 10 L min ⁻¹ , Cold water: 30 L min ⁻¹					
70	5524	4959	2161	26.2	0.6398
60	5255	4959	2119	17.8	0.7137
50	5110	4959	2095	13.1	0.7070

3.1 Concentration of CMC – 0.2%, 0.4%, 0.6%

Figure 3 presents the variations in Nusselt numbers

divided by cube roots of Prandtl numbers as functions of relatively low Reynolds numbers for 0.2%, 0.4% and 0.6% concentration CMC solutions. As shown in the figure, the exponents of Reynolds number are 1.042, 0.633 and 0.847, respectively. This indicates that the relationship between Nusselt number and Reynolds number may very well be considered as linear for 0.2% concentration of CMC, with other cases being logarithmic. Figure 4 presents the variations in friction factors as functions of Reynolds numbers. Examination of non-linear relationships between friction factor and Reynolds Number revealed *R*² values of 0.764, 0.832 and 0.862 for 0.2%, 0.4% and 0.6% concentrations. Exponents of Reynolds numbers for the friction factors are –0.87, –0.95 and –1.08, respectively.

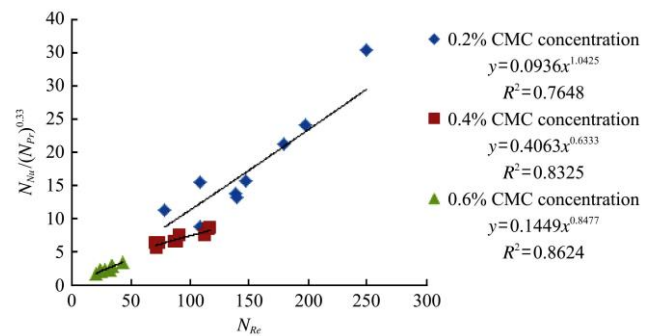


Figure 3 Nusselt/Reynolds numbers' plots for 0.2%, 0.4% and 0.6% CMC concentrations

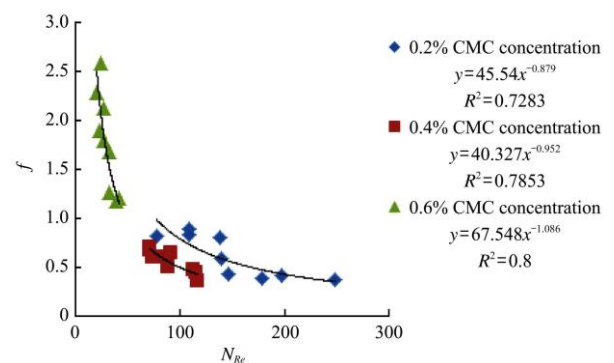


Figure 4 Friction factor (*f*)/Reynolds numbers' plots for 0.2%, 0.4% and 0.6% CMC concentrations

Table 3 lists the values of correlation constants, *a*, *b*, *c* and *d*, as obtained from the following arrangements, as given inper Equation (14) and Equation (15):

$$\text{Log} (N_{Nu}) = \text{log} (a) + b \text{log} (N_{Re}) + 0.33 \text{log} (N_{Pr}) \quad (14)$$

$$\text{And, } \text{log} (f) = \text{log} (c) + d \text{log} (N_{Re}) \quad (15)$$

Either equation was used to formulate three pairs based on three inlet temperatures of hot CMC solutions: 50 °C, 60 °C and 70 °C. The three pairs of equations were

solved for obtaining a and b from Equation (14) and c and d from Equation (15). The resultant mean values of a , b , c and d are listed in Table 3.

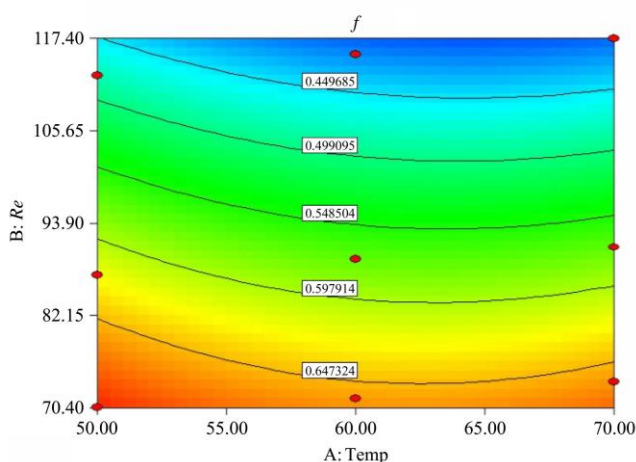
Table 3 Correlation constants

CMC concentration	a	b	c	d
0.2%	0.0936	1.0425	45.54	-0.879
0.4%	0.4063	0.6333	40.327	-0.952
0.6%	0.1450	0.8477	67.548	-1.086

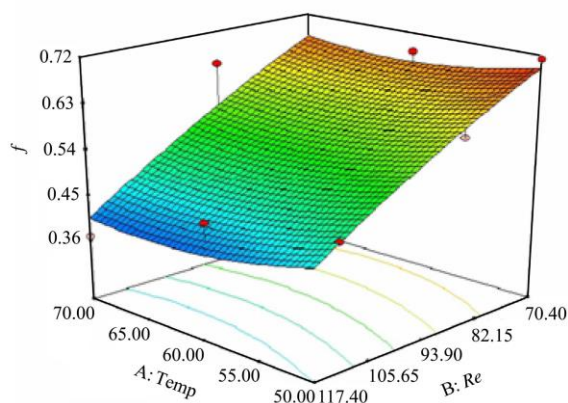
3.2 Effect of variation of temperature and flow rate on friction factor

To confirm the significant effect of temperature and flow rate of solution on friction factor, 3D contour and

plot are obtained in Figure 5 among inlet temperature, Reynolds number and friction factor (for 0.4% CMC concentration). From contour, it can be seen that colour gradient of friction factor f along the temperature axis is very negligible as compared to gradient along Reynolds Number Re axis. Difference in the slope of variation of friction factor along two remaining axes can be easily visualized in 3D plot. Effect of variation of inlet temperature of fluid on f is negligible for the given range of temperature. But change in f is considerable for change in fluid flow rate. The same result can be seen for other remaining CMC concentrations.



a. 3D Contour



b. 3D Plot friction factor/Temperature and Reynolds number

Figure 5 Variation of friction factor as function of temperature and Reynolds number

3.3 Overall heat transfer coefficient for water and CMC solution

It can be seen from Figure 6 that there is drastic drop in heat transfer coefficient of solution from that of water. This effect is due to apparent viscosity of non-Newtonian fluid. Because of high viscosity, heat transfer coefficient is reduced by almost 50%. Similar variations were observed for other concentrations of CMC solution.

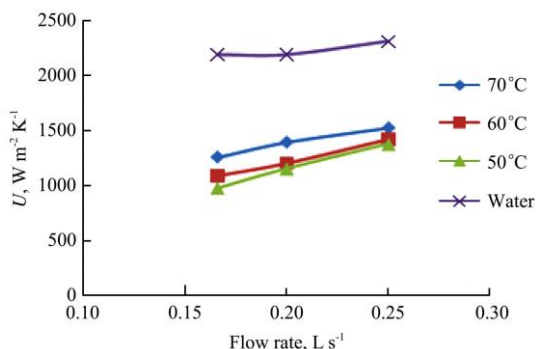


Figure 6 Comparison of overall heat transfer coefficient between water and 0.4% CMC solution

3.4 Simulation of fluid flow

2D sketch of heat exchanger plate is drawn in Figure 7 using software Gambit 2.2.

Grid is generated in Figure 8 using meshing tool in Gambit. Interval size is kept as 0.3 and quadrilateral element shape is used. Different sections of plates are assigned in different boundary conditions. Left entry is taken as fluid INLET and right exit is taken as fluid OUTLET. Upper plate is taken as WALL1 and lower plate is taken as WALL2. This bound region forms the passage for the flow of fluid. Through this passage, flow is simulated using FLUENT 6.3 software specifying experimental conditions.

Though inlet velocity for each concentration is kept at a particular level, due to corrugation over plate, velocity is varying within particular ranges. This creates local turbulence effect at bends and corners which increases local heat transfer coefficient. Figures 9-11 present

simulations for 0.2%, 0.4% and 0.6% concentration CMC solutions. Table 4 enlists the inlet, maximum and

minimum velocities, as obtained from the simulations of various CMC solutions flow through the plates.

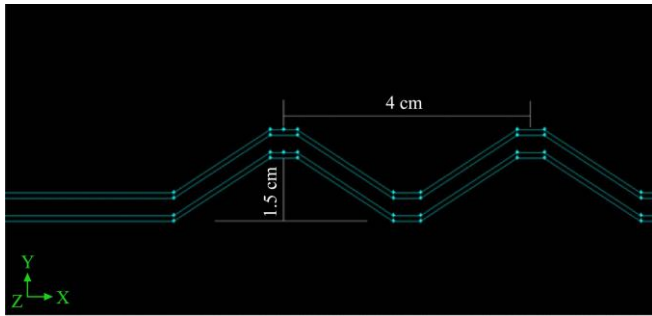


Figure 7 Plate geometry details

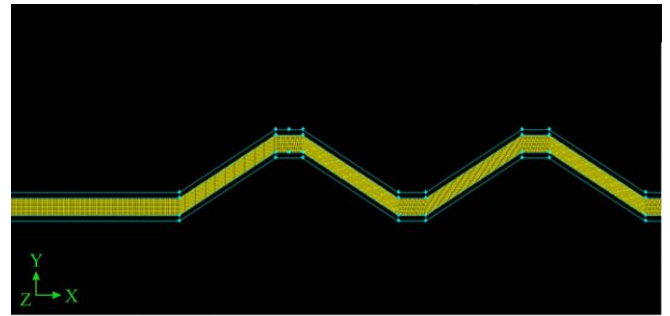


Figure 8 Grid structure of fluid path

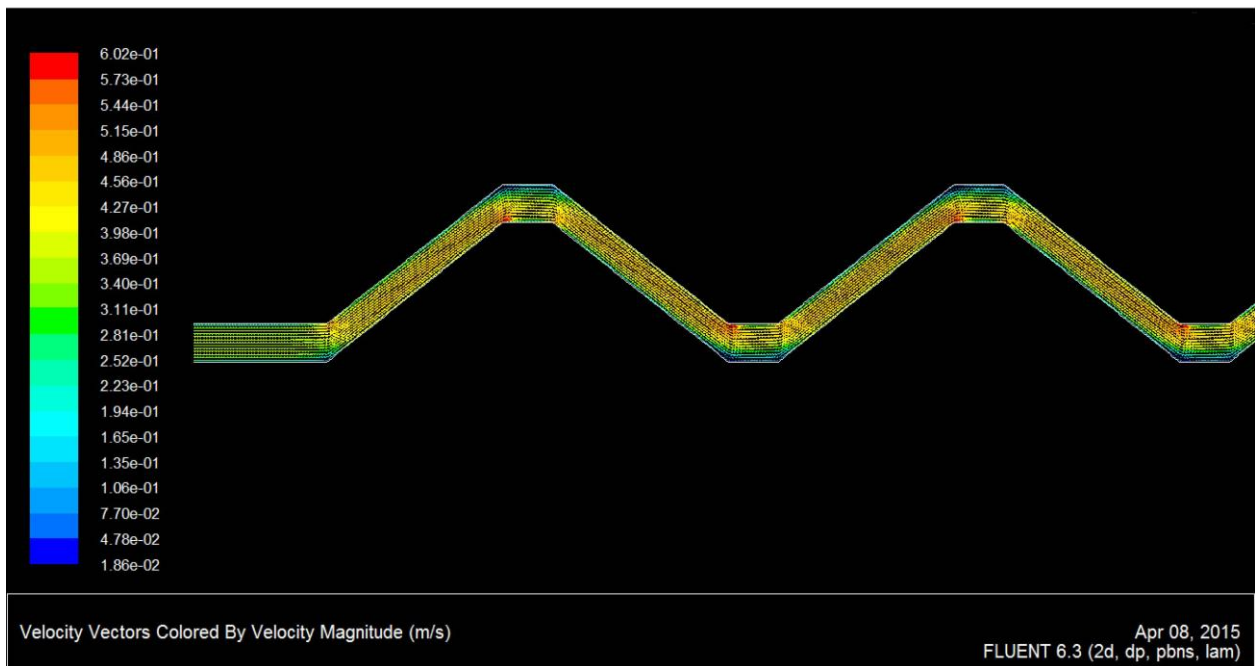


Figure 9 Simulation of 0.2% CMC solution with inlet velocity 0.333 m s^{-1} (20 L min^{-1})

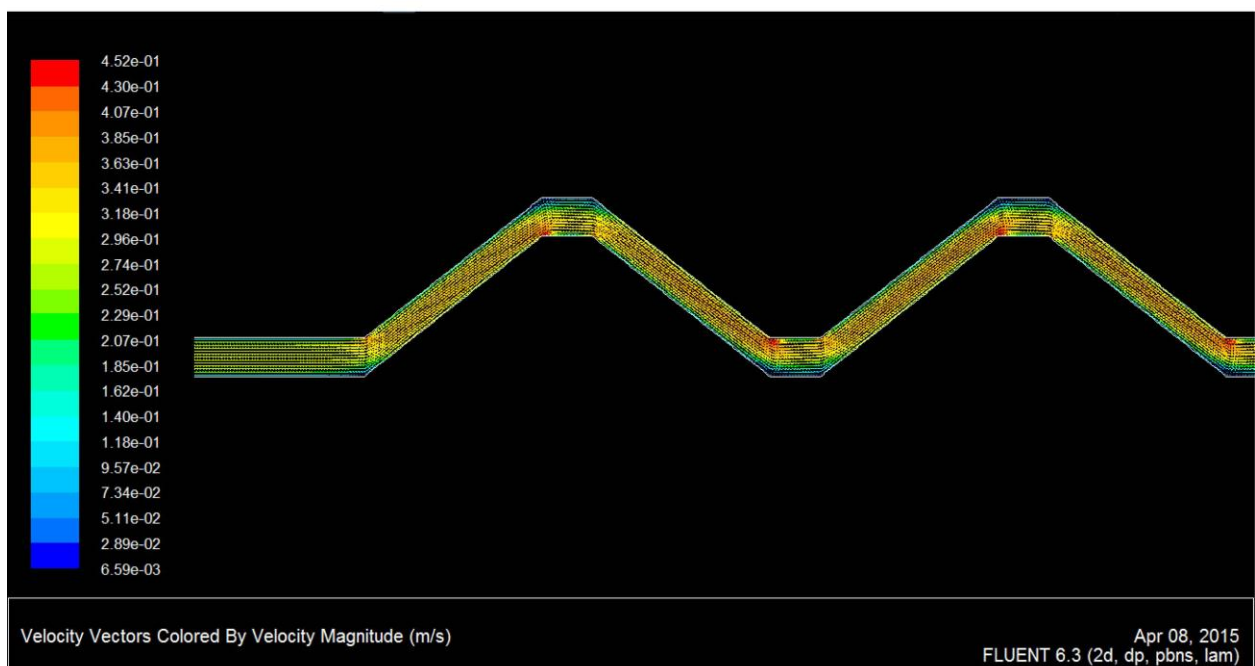


Figure 10 Simulation of 0.4% CMC solution with inlet velocity 0.25 m s^{-1} (15 L min^{-1})

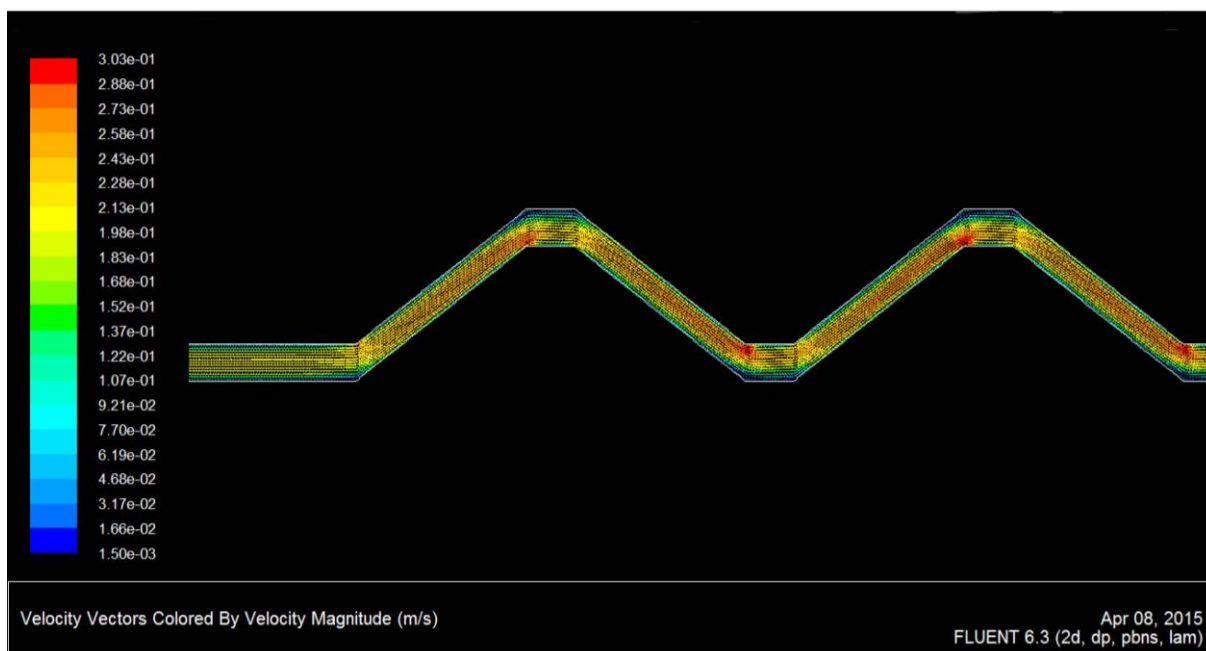


Figure 11 Simulation of 0.6% CMC solution with inlet velocity 0.166 m s^{-1} (10 L min^{-1})

Table 4 Range of velocity variation due to corrugation

CMC Concentration	Inlet velocity, m s^{-1}	Maximum velocity, m s^{-1}	Minimum velocity, m s^{-1}
0.2%	0.333	0.602	0.018
0.4%	0.250	0.452	0.007
0.6%	0.166	0.303	0.002

We can observe reversal of flow pattern at the leading edge of corrugation (Figure 12). The same effect can be seen for complete edge of corrugation as the tendency of fluid is to get stagnant in this section. This result is analogous with the results obtained by Muley et al. (1999).

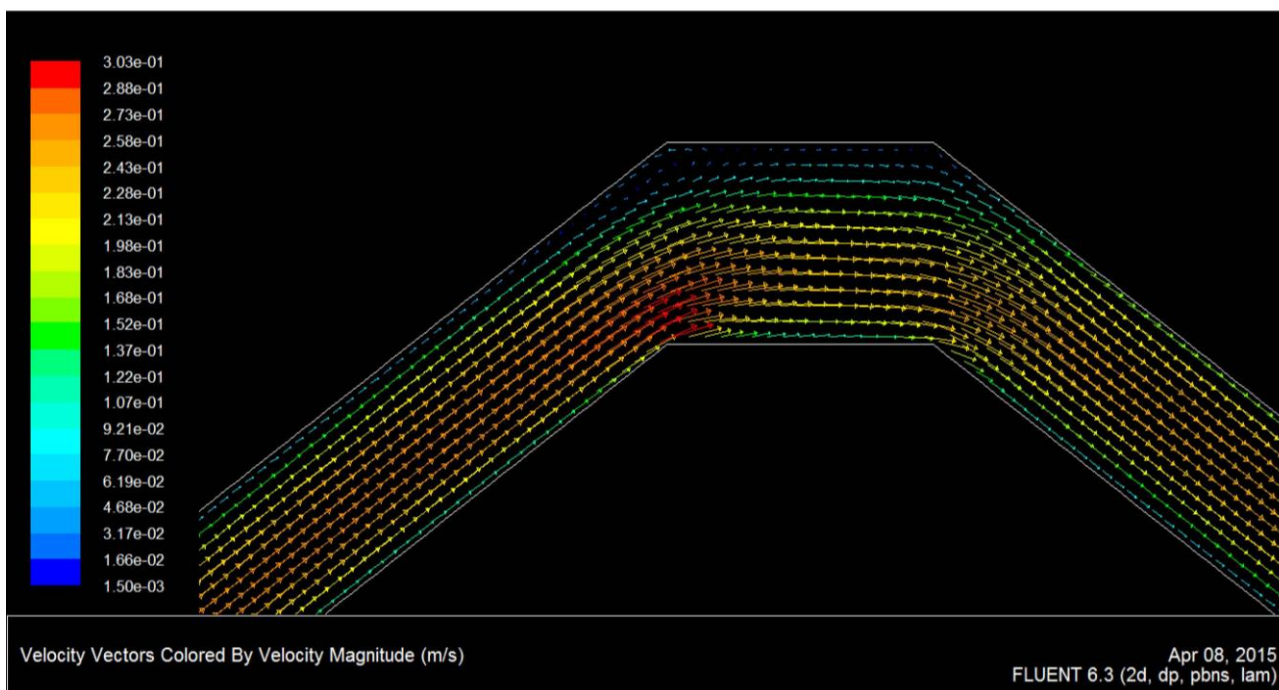


Figure 12 Flow reversal pattern for high viscous fluids

3.5 Prediction of intermediate temperatures of fluid (theoretical approach)

It is very difficult to find out the temperature of fluid at the end of each and every plate of the heat exchanger as the entire setup is tightly compacted. The need to insert

thermocouples for accurate measurement of temperature may lead to leakage from the system. Following is one theoretical approach which was implemented to estimate intermediate temperatures.

Considering the case of 0.2% CMC solution with a

flow rate of 20 L min⁻¹, experimental inlet & outlet temperatures of both of the fluids are known and shown

in the Figure 13 along with the direction of heat transfer among fluids across each plate.

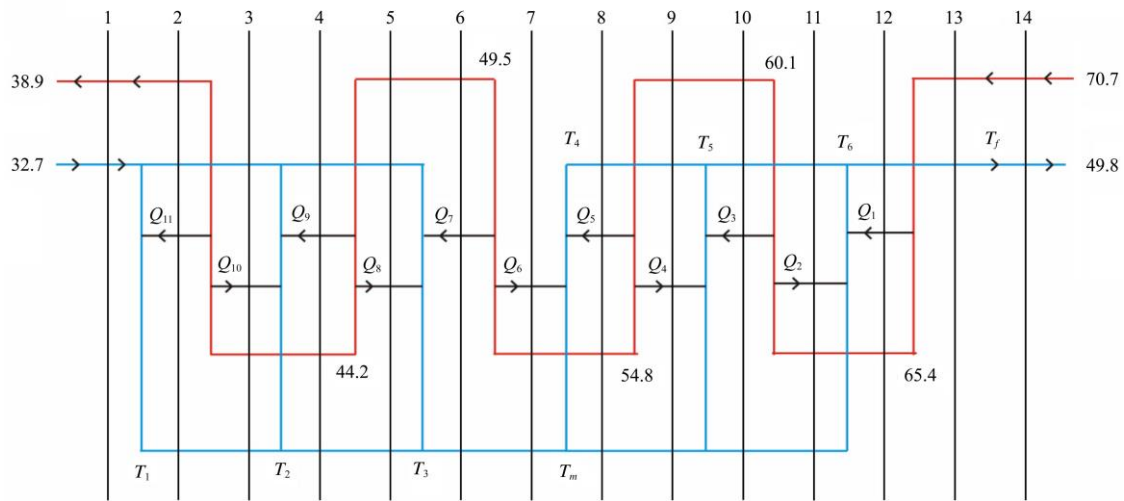


Figure 13 Heat transfer across each plate

Temperature of hot solution after each pass can be obtained by linear interpolation. (dividing net temperature difference by number of passes, i.e. six). Table 5 lists and Figure 14 represents the intermediate temperatures after each pass.

temperatures for PHEs. Figure 15 shows the temperature distribution across plates.

Table 5 Temperature of hot solution after each pass

Pass (Channel)	0	1	2	3	4	5	6
Temperature, °C	70.7	65.4	60.1	54.8	49.5	44.2	38.9

Calculated final temperature ($T_f = 49.82\text{ °C}$) and experimentally obtained temperature ($T_{co} = 49.8\text{ °C}$) are very close. Hence assumptions regarding heat transfer are valid. This approach can be used to calculate intermediate

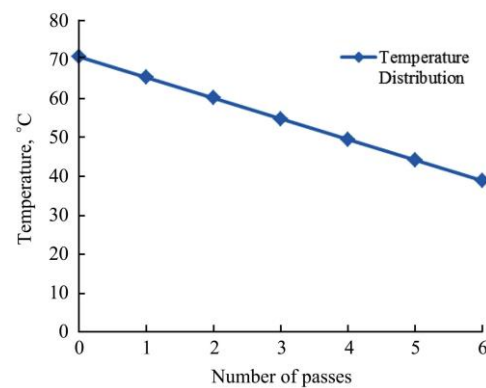


Figure 14 Linear interpolation of temperature of hot solution

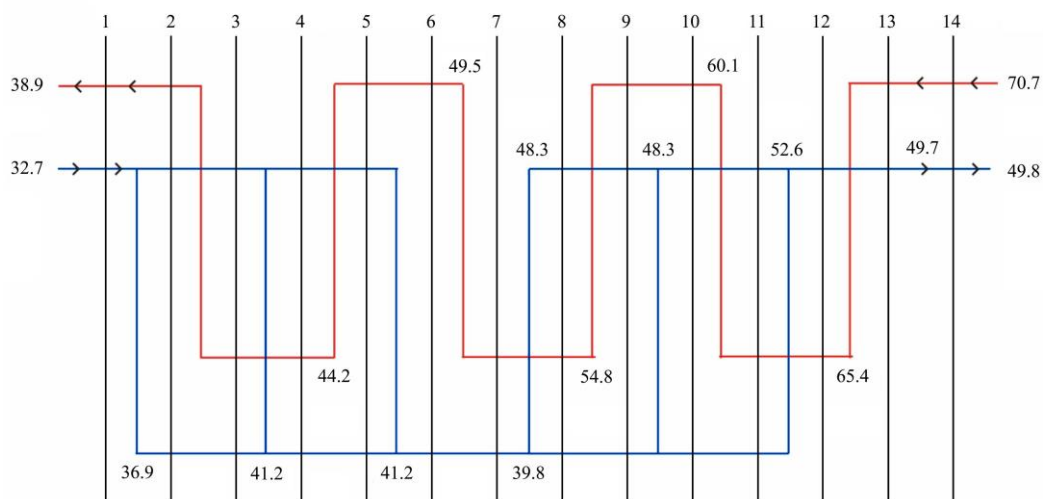


Figure 15 Temperature distribution across plates

4 Conclusions

From the study it is very clear that if PHEs are

designed simply on the basis of Newtonian fluid (water) for different food materials, the system will be underdesigned and the required amount of heat duty

cannot be achieved. In addition to this, heat transfer correlations established for Newtonian fluids cannot be used for pseudoplastic fluids. New equations should be used for food materials having the same properties as that of the mentioned concentrations of solutions.

- 0.7 was taken as the mean log – mean temperature correction factor for the plate heat exchanger, as obtained from the analysis.

- The exponents of Reynolds number for 0.2%, 0.4% and 0.6% CMC solutions are 1.042, 0.633 and 0.847, respectively for expressing Nusselt numbers divided by the cube root of Prandtl numbers.

- Exponents of Reynolds numbers for the friction factors for the same concentrations of CMC are –0.87, –0.95 and –1.08, respectively.

- As the flow rate of fluid goes on increasing, friction factor goes on decreasing. At higher flow rate, fluid experiences more resistance from fluid itself due to velocity gradient than that from solid surface.

- Because of corrugations made on plates, fluid velocity does not remain constant throughout. It varies from low to high value. Hence local heat transfer coefficient is increased at places of higher velocity which enhances indirect heat exchange.

- For high viscous fluid along the corrugations, flow reversal can take place which leads to stagnation zones in fluid flow. Because of this, heat transfer in such zones may decrease as there is very little fluid movement. Corrugations should be designed considering this demerit.

- Simulation can turn out to be an effective tool to optimize plate design before actual manufacturing of the plates.

- Theoretical approach can be used to predict intermediate temperature distribution of fluids along the plates of heat exchanger.

Appendix – Computation for estimation of intermediate temperatures in the plates

Heat transferred by hot solution is given by

$$Q_h = (q_h \times \rho_h) \times Cp_h \times (T_{hi} - T_{ho})$$

$$Q_h = (0.333 \times 10^{-3} \times 973) \times 4.036 \times (70.7 - 38.9)$$

$$Q_h = 41.585 \text{ kW}$$

As the hot solution passes through the six channels, it is reasonable to assume that it transfers equal amount of heat in each channel. So heat transferred by hot fluid in each channel is

$$Q_{hp} = Q_h / 6$$

$$Q_{hp} = 6.931 \text{ kW}$$

Out of this transferred heat, some heat is lost to the surrounding and only part of it is gained by cold fluid. It is important to know the exact amount gained by cold fluid as we are interested in estimating intermediate temperatures.

Total heat gained by cold water

$$Q_c = (q_c \times \rho_c) \times Cp_c \times (T_{co} - T_{ci})$$

$$Q_c = (0.5 \times 10^{-3} \times 992.2) \times 4.182 \times (49.8 - 32.7)$$

$$Q_c = 35.477 \text{ kW}$$

Factor by which part of heat gained by cold water from hot solution

$$z = Q_c / Q_h$$

$$z = 35.477 / 41.585$$

$$z = 0.853$$

Hence, heat received by the cold water per pass of hot water is

$$Q_{cp} = Q_{hp} \times z$$

$$Q_{cp} = 6.931 \times 0.853$$

$$Q_{cp} = 5.912 \text{ kW}$$

From the figure of heat transfer, we can see that

$$Q_{cp} = Q_1 = Q_2 + Q_3 = Q_4 + Q_5 = Q_6 + Q_7 = Q_8 + Q_9$$

$$= Q_{10} + Q_{11} = 5.912 \text{ kW}$$

Now let us assume that hot solution transfers equal amount of heat to side plates through which it is flowing.

Then heat gained by cold fluid are

$$Q_1 = 5.912 \text{ kW}$$

$$Q_2 = Q_3 = Q_4 = Q_5 = Q_6 = Q_7 = Q_8 = Q_9 = Q_{10} = Q_{11} = Q_{cp} / 2$$

$$= 2.956 \text{ kW}$$

From the figure of temperature distribution

$$Q_{11} = (q_c / 3) \times \rho_c \times Cp_c \times (T_1 - 32.7)$$

$$2.956 = (0.166 \times 10^{-3} \times 992.2) \times 4.182 \times (T_1 - 32.7)$$

$$T_1 = 36.99 \text{ }^\circ\text{C}$$

$$Q_9 + Q_{10} = (q_c / 3) \times \rho_c \times Cp_c \times (T_2 - 32.7)$$

$$5.912 = (0.166 \times 10^{-3} \times 992.2) \times 4.182 \times (T_2 - 32.7)$$

$$T_2 = 41.28 \text{ }^\circ\text{C}$$

The same condition for T_3

$$T_3 = 41.28 \text{ }^\circ\text{C}$$

Applying energy balance at the point of mixing of 1st pass of cold water

$$m_1 \times Cp_c \times (T_m - T_1) = m_2 \times Cp_c \times (T_2 - T_m)$$

$$0.166 \times (T_m - 36.99) = 0.332 \times (41.28 - T_m)$$

$$T_m = 39.85 \text{ }^\circ\text{C}$$

$$Q_5 + Q_6 = (q_c/3) \times \rho_c \times Cp_c \times (T_4 - T_m)$$

$$5.912 = (0.166 \times 10^{-3} \times 992.2) \times 4.182 \times (T_4 - 39.81)$$

$$T_4 = 48.39 \text{ }^\circ\text{C}$$

The same condition for T_5

$$T_5 = 48.39 \text{ }^\circ\text{C}$$

$$Q_1 + Q_2 = (q_c/3) \times \rho_c \times Cp_c \times (T_6 - T_m)$$

$$8.868 = (0.166 \times 10^{-3} \times 992.2) \times 4.182 \times (T_6 - 39.81)$$

$$T_6 = 52.69 \text{ }^\circ\text{C}$$

Applying energy balance at the point of mixing of 2nd pass of cold water

$$m_2 \times Cp_c \times (T_f - T_5) = m_1 \times Cp_c \times (T_6 - T_f)$$

$$0.332 \times (T_f - 48.39) = 0.166 \times (52.69 - T_f)$$

$$T_f = 49.82 \text{ }^\circ\text{C}$$

List of Abbreviations:

CMC Carboxymethylcellulose

Cp Specific heat capacity ($\text{kJ kg}^{-1} \text{K}^{-1}$)

D_h Hydraulic diameter (m)

f friction factor (dimensionless)

F LMTD correction factor (dimensionless)

h_c Cold fluid side heat transfer coefficient ($\text{W m}^{-2} \text{K}^{-1}$)

h_h Hot fluid side heat transfer coefficient ($\text{W m}^{-2} \text{K}^{-1}$)

K Consistency coefficient (Pa s^n)

k_h Thermal conductivity of hot fluid ($\text{W m}^{-1} \text{K}^{-1}$)

k_m Thermal conductivity of metal plates ($\text{W m}^{-1} \text{K}^{-1}$)

L Length (m)

n Flow behavior index (dimensionless)

Nu_{th} Hot fluid side Nusselt number (dimensionless)

Pr_h Hot fluid side Prandtl number (dimensionless)

q flow rate ($\text{m}^3 \text{s}^{-1}$)

Q_h Heat lost by hot fluid (W)

Re_h Hot fluid side Reynolds number (dimensionless)

t Thickness of metal plate (m)

T_{ci} Cold water inlet temperature ($^\circ\text{C}$)

T_{co} Cold water outlet temperature ($^\circ\text{C}$)

T_{hi} Hot fluid inlet temperature ($^\circ\text{C}$)

T_{ho} Hot fluid outlet temperature ($^\circ\text{C}$)

T_{lm} Logarithmic mean temperature difference LMTD ($^\circ\text{C}$)

U Overall heat transfer coefficient ($\text{W m}^{-2} \text{K}^{-1}$)

$\dot{\gamma}$ Shear rate (s^{-1})

Greek Symbols

δ Half-thickness of gap between two plates (m)

ΔP Pressure drop (Pa)

ρ Density (kg m^{-3})

τ Shear stress (Pa)

References

- Bereiziat, D, and R. Devienne. 1999. Experimental characterization of Newtonian and non-Newtonian fluid flows in corrugated channels. *International Journal of Engineering Science*, 37(11): 1461–1479.
- Fernandes, C. S., F., R. P. Dias, J. M. Nobrega, and J. M. Maria. 2007. Laminar flow in chevron-type heat exchangers: CFD analysis of tortuosity, shape factor and friction factor. *Chemical Engineering and Processing: Process Intensification*, 46(9): 825–833.
- Datta, A. K. 2001. *Transport Phenomena in Food Process Engineering*. Mumbai, India: Himalaya Publishing House, Mumbai.
- Gradeck, M., B. Hoareau, and M. Lebouche. 2005. Local analysis of heat transfer inside corrugated channel. *International Journal of Heat and Mass Transfer*, 48(10): 1909–1915.
- Kumar A. 2006. Measurement of thermo physical properties of non-Newtonian fluid (CMC); Unpublished. M. Tech. Thesis. Agricultural and Food Engineering Department, IIT Kharagpur.
- Kumbhare, M. B., and S. D. Dawande. 2013. Performance evaluation of plate heat exchanger in laminar and turbulent flow conditions. *International Journal of Chemical Sciences and Applications*, 4(1): 77–83.
- Muley, A., R. M. Manglik, and H. M. Metwally. 1999. Enhanced heat transfer characteristics of viscous liquid flows in a chevron plate heat exchanger. *Journal of Heat Transfer*, 121(4): 1011–1017.